Heliyon 11 (2025) e42183

Contents lists available at ScienceDirect

Heliyon

journal homepage: www.cell.com/heliyon

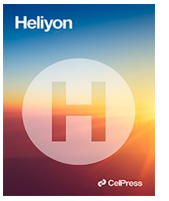

Research article

Integrated and streamlined microfluidic device for molecular diagnosis of pathogen through direct PCR amplification

Dohwan Lee [a,*], Tae Seok Seo [b,**]

[a] Department of Electrical Engineering, Kwangwoon University, Seoul, 01897, Republic of Korea
[b] Department of Chemical Engineering (BK21 FOUR Integrated Engineering Program), Kyung Hee University, Yongin, 17104, Republic of Korea

A B S T R A C T

Background: Polymerase chain reaction (PCR) is a gold-standard method widely acknowledged for offering precise and rapid analysis of genetic material, particularly having a crucial role in detecting pathogens and diagnosing infectious diseases. However, the complexity of the PCR process (including nucleic acid extraction/purification, amplification, and amplicon detection) hinders its widespread adoption in point-of-care testing, where simplicity and rapidity are essential for practical use.

Results: In this study, we developed a microfluidic genetic analysis device that leverages direct PCR technology to simplify the entire PCR process, focusing on enhancing the usability and accessibility of the device for point-of-care diagnostics. Direct PCR, which enables direct DNA amplification from biological samples without the need for DNA extraction and purification, streamlines the device architecture and transforms it into a more user-friendly form. Within the device, two spatially separated zones for PCR and micro-capillary electrophoresis (μCE) are sequentially connected via a microchamber plate, which is slidable on top of the device and transfers the amplified products from the PCR zone to the μCE zone for subsequent analysis. Using our device, we quantitatively analyzed two types of bacteria—*Escherichia coli* (*E. coli*) and *Staphylococcus aureus* (*S. aureus*)—in milk (food poisoning simulation) with a sensitivity of up to 10 bacterial cells.

Significance: Considering how prominent PCR is for diagnostics, this work represents the potential to make traditionally labor-intensive molecular assays available in a decentralized point-of-care setting.

1. Introduction

Polymerase chain reaction (PCR) is a gold-standard method widely used to amplify minute quantities of DNA, transforming the landscape of molecular biology and biomedical diagnostics [1–6]. The significance of PCR has become even more pronounced following consecutive COVID-19 pandemic waves, highlighting its vital role in accurate testing, transmission tracking/monitoring, and follow-up care [1–6]. This escalation in importance underscores the PCR's transformation into a universally recognized and essential tool for biomedical research, diagnostics, and biosensor applications, transcending its previous academic and specialized confines to becoming an integral part of everyday healthcare practices [6–9].

The ubiquity of PCR has spurred attempts to adapt it to point-of-care (POC) testing for simple and immediate diagnosis of diseases [10–16]. Microfluidics, which is characterized by the manipulation of small volumes of fluids (such as biological samples, assay buffers, and reagents) within a micron-sized device, has emerged as a promising platform for this purpose. Leveraging its portability, low power and reagent consumption, rapid analysis, and user-friendliness [17–20], researchers have harnessed the full potential of PCR by embedding it in microfluidic devices that rapidly and accurately detect target analytes at the site of patient care, circumventing the delays and complexities associated with traditional centralized laboratory-based diagnostics [14–16].

* Corresponding author.
** Corresponding author.
E-mail addresses: dlee@kw.ac.kr (D. Lee), seots@khu.ac.kr (T.S. Seo).

https://doi.org/10.1016/j.heliyon.2025.e42183
Received 22 August 2024; Received in revised form 9 January 2025; Accepted 21 January 2025
Available online 22 January 2025
2405-8440/© 2025 The Authors. Published by Elsevier Ltd. This is an open access article under the CC BY-NC license (http://creativecommons.org/licenses/by-nc/4.0/).

Despite these efforts, adapting the PCR process to microfluidic devices poses significant challenges, predominantly because of the complex PCR steps involved: 1) nucleic acid extraction and purification from a sample, 2) PCR amplification, and 3) amplicon analysis. These steps typically include multiple buffer changes and washing steps, making microfluidic devices less accessible to non-specialists and limiting their deployment outside of sophisticated laboratories [5,19]. Moreover, integrating these individual steps (steps 1–3) into a single device is far from trivial given the sophistication and sensitivity inherent in the PCR process, which precludes the possibility of bypassing or dispensing with any step. Often, microfluidic PCR devices achieve miniaturization at the expense of operational simplicity [21–24] but require external pumps and intricate valve structures to manipulate fluid movement. This paradoxically aligns them more with the "Chip in a Lab" concept rather than achieving true point-of-care testing in decentralized settings [25–28].

To address these challenges, we report a new approach that combines the advantages of microfluidic devices with those of direct PCR technology. Direct PCR, capable of amplifying DNA directly from biological samples without DNA extraction and purification steps while mitigating PCR inhibitors [29–34], has the potential to streamline the PCR process, consequently, we can simplify the microfluidic device architecture, significantly minimizing the reliance on complex valve systems, tubing, and external pumps. Furthermore, we incorporated our previous slidable microchamber techniques [17,29], which enabled the transfer of the PCR products from the spatially separated PCR zone to a micro-capillary electrophoresis (μCE) zone for subsequent amplicon analysis. Using our genetic analysis device, we detected and quantified two bacteria, *Escherichia coli* (*E. coli*) and *Staphylococcus aureus* (*S. aureus*), contaminated in milk (food poisoning simulation).

2. Materials and methods

2.1. Direct PCR technology

Direct PCR is an innovative technique that streamlines the traditionally complex PCR process by eliminating the nucleic acid extraction and purification steps, which are often labor-intensive and time-consuming. Conventional PCR processes, involving multiple steps of sample collection, sample lysis, nucleic acid extraction, and elution, take several hours to complete (Fig. 1a). In contrast, direct PCR allows the direct use of untreated biological samples (such as blood, tissue, or food samples) in PCR amplification, bypassing the painstaking DNA preparation steps. A critical feature of direct PCR is its ability to overcome the inhibitory effects of substances present in complex biological matrices, such as calcium ions, lipids, and proteins found in milk or hemoglobin in blood. These inhibitors are addressed through specially formulated reaction buffers containing components such as bovine serum albumin, which stabilizes DNA polymerase by binding to inhibitory substances, detergents that disrupt cell membranes and mitigate hydrophobic

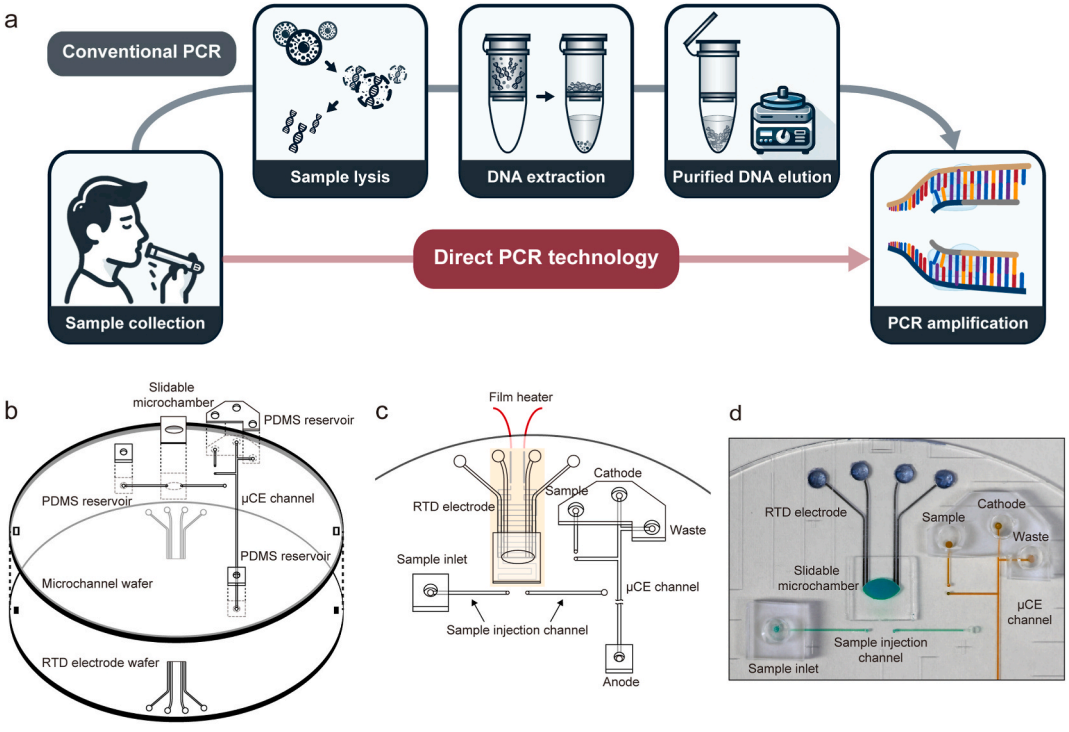

Fig. 1. Genetic analysis device incorporated with the direct PCR technology. (a) Conventional versus direct PCR procedures. (b) Exploded view of the device. The device comprises an RTD electrode wafer, a microchannel wafer, a slidable microchamber, and three PDMS reservoirs. (c) Schematic of all device components assembled, and (d) photograph of the genetic analysis device, taken from the top, showing the PCR reagent (green dye) introduced into the slidable microchamber through the sample injection channel and isolated by sliding up the microchamber.

inhibitors, and chelating agents that sequester divalent cations such as calcium [30,31]. Robust DNA polymerases, specially engineered for their high tolerance to inhibitors, also ensure consistent and efficient amplification under challenging conditions. By combining these features, direct PCR enables reliable and rapid DNA amplification across a wide range of sample types. In addition, direct PCR minimizes the risk of sample contamination and loss of material, all of which offer a practical solution to the demands of high-throughput and POC applications.

2.2. Design of genetic analysis device

The genetic analysis device primarily comprised two 4-inch glass wafers, a slidable microchamber, and polydimethylsiloxane (PDMS) reservoirs (exploded view of the device, Fig. 1b). A four-point resistance temperature detector (RTD) electrode (2 nm Ti and 200 nm Pt) was deposited on the upper side of the bottom wafer (called the RTD electrode wafer) for real-time temperature measurements. The microchannels with dimensions of 140 μm width and 100 μm depth were patterned on the bottom side of the upper wafer (called microchannel wafer) for sample injection and CE operation (see detailed dimensions of microchannels, Fig. S1). A concaved micro-reactor of 2 μl was fabricated on the bottom side of the slidable microchamber (10 mm × 10 mm × 0.5 mm). Three PDMS reservoirs were attached to the upper side of the microchannel wafer. A schematic image (Fig. 1c) and a top-view photograph of the genetic analysis device taken from the top (Fig. 1d) display all the device components assembled. The sample injection and μCE channels were spatially disconnected, but they can sequentially be connected by placing and moving the slidable microchamber. This allows PCR reagents to be easily: 1) introduced into the slidable microchamber through the sample injection channel, 2) isolated for PCR on top of the RTD electrode and the film heater, and 3) transferred to the μCE channel for genetic analysis. In the photograph of the device (Fig. 1d), the sample injection channel and 2 μL micro-reactor in the slidable microchamber were filled with a green dye, and the μCE channel was filled with a yellow dye.

2.3. Device fabrication

The genetic analysis device was fabricated using a microfabrication technique described in a previous study [17]. To fabricate the RTD electrode wafer, Ti (20 nm) and Pt (200 nm) layers were coated onto a 4-inch borofloat glass wafer surface (PG&O, CA, USA) by sputtering. The coated wafer surface was primed with hexamethyldisilazane (HMDS) to promote photoresist adhesion. A positive photoresist (Shipley1818, Rohm and Haas Electronic Materials LLC, MA, USA) was then spin-coated onto the Ti/Pt wafer surface and soft-baked at 120 °C for 90 s. The RTD electrode patterns were transferred to a photoresist by using a film mask under UV exposure. The UV-exposed region of the photoresist was washed with a Microposit developer (1:1 with deionized water; Rohm and Haas Electronic Materials LLC). The revealed Ti/Pt layer (unprotected by photoresist) was etched by immersing the wafer in an aqua regia solution (HCl: HNO3 = 3:1) at 90 °C and the remaining photoresist (on top of the RTD electrode pattern) was removed with acetone. To fabricate the microchannel wafer, 200 nm of amorphous silicon (α-si) was coated on a 4-inch borofloat glass wafer through LPCVD. After priming with HMDS, the positive photoresist was spin-coated and soft-baked at 120 °C for 90 s. The microchannel design was then transferred to a photoresist through a film mask with UV exposure, and the exposed photoresist was removed using the developer. The revealed α-si layer (unprotected by photoresist) was dry-etched anisotropically by SF_6 reactive ion etching (RIE), and the exposed glass surface was wet-etched isotropically using 49 % hydrofluoric acid, which forms 100 μm microchannels on the wafer surface. The remaining photoresist and α-si layers were washed away with acetone and KOH solutions, respectively. Holes (1 mm in diameter) were drilled into the microchannel wafer using a CNC milling machine. The slidable microchamber with 2 μl of a concaved micro-reactor was fabricated in the same manner and diced to a size of 10 mm × 10 mm. Both the RTD electrode and microchannel wafers were thoroughly cleaned with a piranha solution and thermally bonded in a vacuum furnace at 668 °C for 5 h. After bonding the two wafers, PDMS reservoirs with a thickness of 5 mm were made and attached to top of the bonded device via oxygen plasma treatment for 5 min. Finally, the surfaces of the fabricated device and the slidable microchamber were rendered hydrophobic using decyltrichlorosilane (DTS) for 1 h in a vacuum chamber.

2.4. Portable genetic analyzer system

To calibrate the fabricated device and perform the genetic analysis, a custom-made portable genetic analyzer system was used, as described in our previous study (Fig. S2) [29,35]. The system integrates all the parts required for genetic analysis: 1) an electronic control board (PCE-e, Nanoscope Systems Inc., Korea) for current/voltage supply and measurement, 2) high-voltage power and laser supplies (AA12-P4, Ultravolt, USA) for CE operation, 3) a cooling fan installed above the PCR zone to facilitate rapid cooling during thermal cycling, 4) a portable fluorescence detector for PCR amplicon analysis, and 5) an in-house LabVIEW program on a laptop to control the entire process. The temperature for PCR thermal cycling was controlled using a PID module within the LabVIEW program. The portable genetic analyzer communicated with the laptop through an RS-232 protocol, with commands sent from the laptop being processed and managed by the FGA-based control board. This control board maintained a constant current, monitored the voltage changes across the RTD sensor, and regulated the heater. The voltage sampling frequency was set to 2 MHz, and every 512 samples were averaged directly on the control board.

2.5. Calibration of the RTD electrode

The newly fabricated device was calibrated prior to use to accurately measure and control the temperature in real-time during PCR

(a key feature for amplifying the gene correctly). For calibration, the device (and RTD electrode) was immersed in a water bath, while the RTD connection pads remained above the water level. The temperature was gradually increased from 25 °C to 70 °C. In the meantime, a constant current of 4 mA was supplied to the outside pair of the RTD electrodes, and the variation in voltage due to the temperature increase was measured through the inside pair of electrodes. The voltage values were recorded every 5 °C, and the measured values were plotted against the applied temperature (Fig. 2a). The relationship between the temperature and measured voltage from the RTD was linear, with a high coefficient of determination ($R^2 = 0.99935$), and a linear regression plot can be expressed by the following equation:

$$Temperature = a + b \times V$$

, where the constants a and b are −260.99 and 315.66, respectively. During PCR amplification, the temperature within the device was estimated using the above equation with voltage change measurements.

After device calibration, we tested PCR thermal cycling (40 cycles) to ensure that the genetic analyzer could appropriately apply the temperature and reaction time, as well as check the temperature ramping and cooling rate on the device (PCR profile on the device, Fig. 2b). We confirmed that the genetic analyzer could apply the correct temperature and incubation time during 40 cycles of PCR with a ramping rate of ~8.4 °C/s and cooling rate of ~4.8 °C/s. The temperature at each PCR step in the device was cross-confirmed using an infrared thermographic camera (Fig. 2c). The measured temperatures from the camera were matched with the target temperatures for denaturation (94 °C), annealing (57 °C), and extension (72 °C).

2.6. Preparation of bacterial cells and milk sample

Escherichia coli (*E. coli*, ATCC 9637) and *Staphylococcus aureus* (*S. aureus*, ATCC 12600) were obtained from the Korean Culture

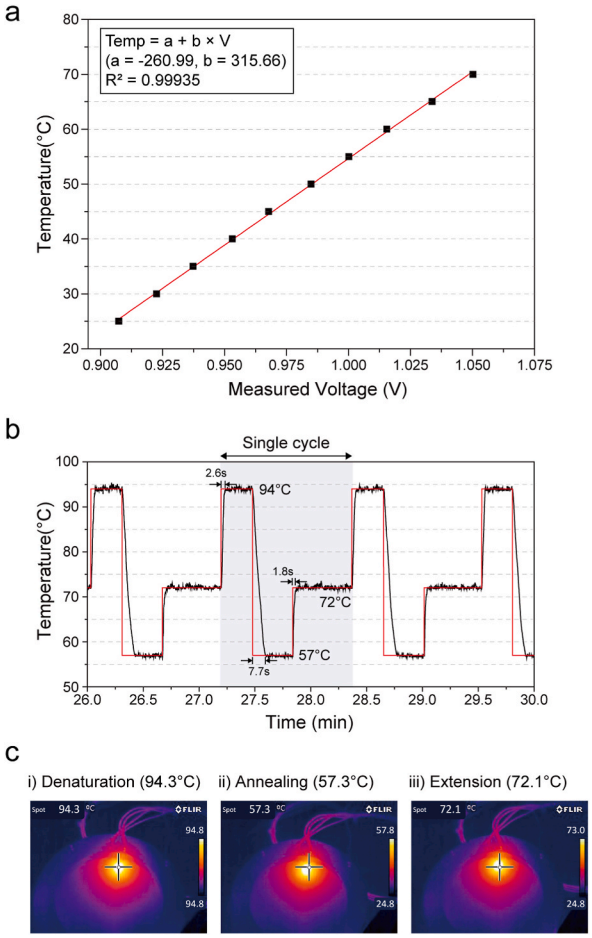

Fig. 2. Calibration of the RTD electrode for PCR thermal cycling. (a) Plot of temperature as a function of the measured voltage from the RTD. The relationship between the temperature and voltage was linear ($R^2 = 0.99935$). (b) PCR thermal cycling profile of the device. The red line represents the preset temperature and the black line represents the actual measured temperature from the device. The ramping rate is ~8.4 °C/s, and the cooling rate is ~4.8 °C/s. (c) Infrared images taken at each PCR step (denaturation at 94.3 °C, annealing at 57.3 °C, and extension at 72.1 °C).

Center of Microorganisms. They were cultured in 10 mL of nutrient broth (0.3 g of beef extract and 0.5 g of peptone in 100 mL of autoclaved water) at 37 °C for 18 h. Cultivated bacterial cells were washed three times with 1x phosphate-buffered saline (PBS), and the number of cells suspended in the buffer was estimated by measuring the absorbance at 600 nm. Milk was purchased from a local grocery market to prepare milk samples contaminated with bacteria, and both bacterial cell types were spiked into the milk. The spiked milk was then serially 10-fold diluted with fresh milk to control the bacterial concentration from 10^4 to 10^2 cells per 2 μL of milk. Spiked milk samples were directly used for direct PCR without DNA extraction and purification.

2.7. Preparation of primer mixture and PCR reagent

PCR primer sequences was described in our previous study [35]. Briefly, the genomic sequences of *E. coli* and *S. aureus* were obtained from GenBank, and PCR primers were designed using Primer3 software (https://bioinfo.ut.ee/primer3-0.4.0/primer3/). The specificity of each primer sequence was verified using a basic local alignment search tool (BLAST). For *E. coli* primer set, the yliE gene was targeted using a forward primer (5′-FAM-TCA AAT AAA TTG CTC TCA CTG AT-3′) and reverse primer (5′-CAC AGC CAG ATA CTG ATT ATT GT-3′). For *S. aureus* primer set, the spA gene was targeted using a forward primer (5′-FAM-ACA AAG CTC AAG CAT TAC CA-3′) and a reverse primer (5′- CGA CGA CGT CCA GCT AAT AA -3′). For real-time quantitative PCR (qPCR), we used identical sequences of primers without FAM tags. The sizes of PCR amplicons were 99 and 112 base pairs for the yliE and spA genes, respectively.

The PCR reagent was prepared with the following composition: 4 μL of 5x EzWay Direct PCR Buffer, 2 μL of dNTP mix (2.5 mM each), 2 μL of primer mixture (2 μM for *E. coli* primer set and 4 μM *S. aureus* primer set), 1 μL of Taq DNA polymerase (5 U/μL), 8 μL of

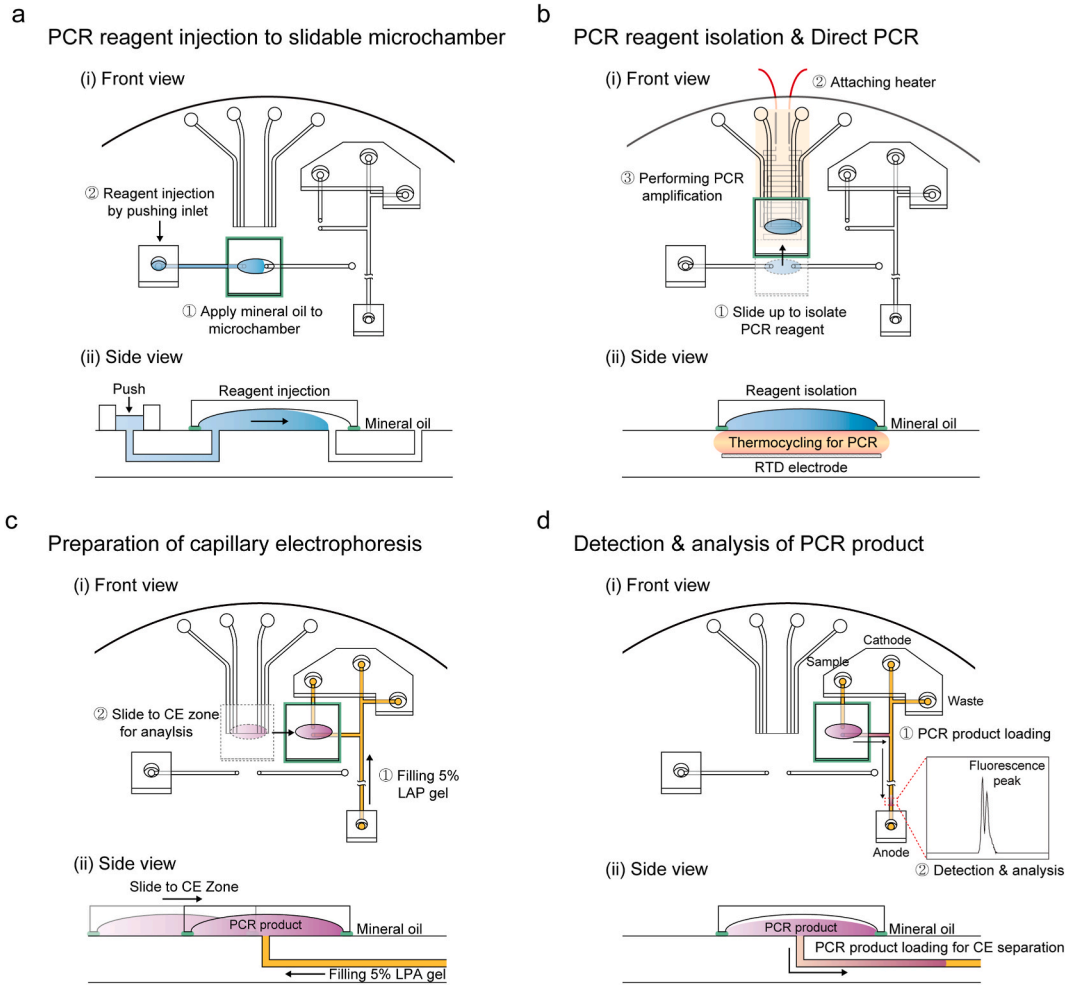

Fig. 3. Operational procedure of the genetic analysis device. (a) The slidable microchamber was aligned between the disconnected sample injection channels, and mineral oil was applied to the periphery of the microchamber to inject 2 μL of the direct PCR reagent into the microchamber by pressing it down on the reservoir. (b) The microchamber was manually slid up to isolate the reagent on top of the RTD electrode and the heater. (c) After completion of the direct PCR, the μCE channel was filled with 5 % LPA and 6 M urea, and the microchamber was slid to connect the spatially disconnected part of the μCE channel. (d) The standard three steps of CE operation were performed by applying high voltages to analyze PCR amplicons from two bacteria.

deionized (DI) water, 1 μL of bovine serum albumin (BSA) solution (2 μg/μL in DI water), and 2 μL of milk sample with each concentration from 10^4 to 10^2 cells per 2 μL. Direct PCR buffer is helpful for the direct lysis of bacterial cell membranes and inactivation of PCR inhibitors in milk (calcium ions, lipids, casein, milk proteins, etc.), which enables direct amplification of DNA fragments from bacterial cells without DNA extraction and purification steps. Primers were obtained from Bioneer (Seoul, South Korea) and all other PCR components were obtained from KOMA Biotech, Inc. (Seoul, South Korea).

2.8. Operation of genetic analysis device

Since the direct PCR technique eliminated the need for cumbersome DNA extraction and purification steps, the device operation was straightforward, and the workflow was streamlined, making it accessible to a broader range of users without training. The operation procedure was identical to that described in our previous study [17]. The slidable microchamber was first aligned between the spatially disconnected sample injection channels to connect them (Fig. 3a). Subsequently, 5 μL of mineral oil was applied to the periphery of the microchamber to prevent leakage and evaporation of the direct PCR reagent during the thermal cycling. 5 μL of the direct PCR reagent was added to the PDMS reservoir, followed by pressing down on the reservoir with a finger to inject 2 μL of the reagent into the micro-reactor within the slidable microchamber. The microchamber filled with the reagent was then manually slid up to isolate the reagent and place it on top of the RTD electrode, and the heater was attached to the bottom of the device (Fig. 3b). Since the surface of the device was treated hydrophobically and mineral oil surrounded the microchamber, no reagent loss or leakage was observed during microchamber movement. Next, the direct PCR thermal cycling was performed using an in-house LabVIEW program as follows: 1) thermal lysis of cells and an initial activation at 95 °C for 5 min; 2) 40 thermal cycles of [95 °C for 5 s, 60 °C for 10 s, and 72 °C for 15 s]; and 3) final extension step at 72 °C for 1 min. After completing the direct PCR, the heater was detached, and the μCE channel was filled with 50 % (v/v) dynamic coating in methanol (The Gel Company, CA, USA) for 3 min to minimize the electroosmotic flow. 5 % linear polyacrylamide (LPA) with 6 M urea as a sieving matrix was then filled in the μCE channel and the microchamber was slid to the CE zone to connect the spatially disconnected part of the μCE channel (Fig. 3c). The μCE channel's temperature was maintained at 70 °C using a silicon rubber heater during the CE operation. To operate the CE for size-based separation and analysis of PCR amplicons, 1 × TTE buffer was added to the PDMS reservoirs (sample, cathode, waste, and anode) and three standard steps of CE operation were performed by applying high voltages to analyze PCR amplicons from two bacteria [36]. 1) A voltage of 1500 V was applied between the sample and waste reservoirs for 120 s to introduce the amplicons into the μCE channel. 2) 2100 V was applied between the anode and cathode reservoirs for 10 s to load the amplicons at the intersection part to a 6 cm-long μCE separation channel, while the voltage at the sample/waste reservoirs was switched to 900 V for back biasing to prevent residual loading. 3) The voltage

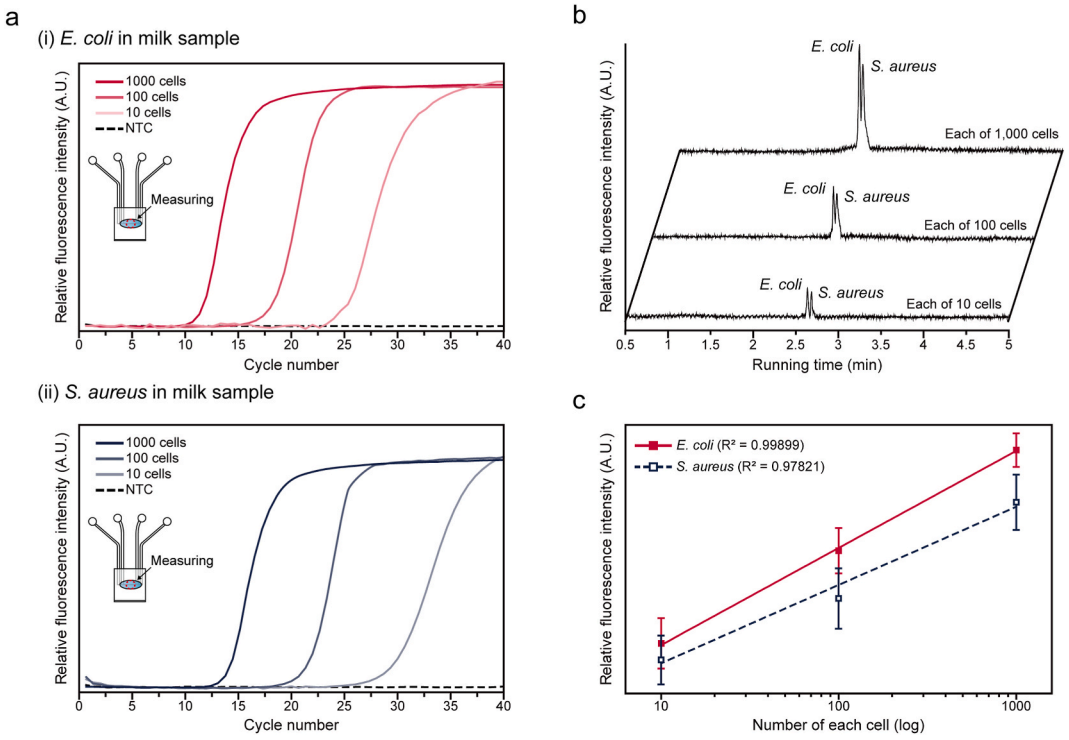

Fig. 4. Detection of *E. coli* and *S. aureus* in milk. (a) The qPCR results obtained using our genetic analysis device from milk samples contaminated with *E. coli* and *S. aureus*. NTC was a negative control tested with milk samples that were not spiked with bacteria. (b) Electropherogram showing multiplex detection of two bacteria with clear separation of PCR amplicons, indicating *E. coli* at ~158 s peak and *S. aureus* at ~161 s peak. (c) Plot showing the measured relative fluorescence intensities as a function of the number of each cell (log).

between the anode and the cathode was switched to 1500 V (250 V/cm) for size-based separation of the PCR amplicons.

2.9. Quantitative data analysis

Fluorescence signals from the PCR amplicons were recorded at the channel's end using a portable fluorescence detector, and the raw data were analyzed using OriginPro software. The fluorescence intensity was plotted against the logarithm of bacterial cell concentration to construct calibration curves for both *E. coli* and *S. aureus*. The detection limits were determined as the lowest cell concentrations producing a signal of three standard deviations above the negative control (NTC). The quantitative range was established by evaluating the linearity of the calibration curves within the tested concentration range (10 to 10^3 cells in 2 μL).

3. Results and discussion

3.1. Detection of E. coli and S. aureus in milk

To demonstrate the capability of our device to detect bacteria in milk samples, we selected *E. coli* and *S. aureus* as representative gram-negative and -positive bacteria, respectively. We prepared milk samples contaminated with these bacteria at concentrations ranging from 10^3 to 10 cells in 2 μL of the direct PCR reagent to mimic food poisoning scenarios. Before multiplex detection of two bacteria using the CE separation, we first performed direct qPCR to confirm that the direct PCR could be executed in 2 μL of the micro-reactor within the microchamber, even without DNA extraction and purification steps. Since the FAM-tagged primers are not suitable for measuring real-time, amplicon-dependent fluorescence signals, we added SYTO-9 dye to the PCR reagent (final concentration: 3.3 μM) during the reagent preparation and used the identical primer sequences without FAM tags for this experiment; the SYTO-9 dye is an intercalating dye that binds specifically to double-stranded DNA.

We recorded the fluorescence intensities in the micro-reactor over 40 cycles of the PCR amplification. We observed successful PCR amplification in the micro-reactor using both *E. coli* and *S. aureus* samples (Fig. 4a). As anticipated, the sample with a higher cell number produced an earlier PCR amplification curve (lower cycle threshold) in both *E. coli* and *S. aureus* samples as well as the amplification of *E. coli* samples at all cell numbers was faster than that of *S. aureus* samples, likely due to the easier thermal lysis of gram-negative bacteria. During qPCR, we did not observe any interference from milk substances to the fluorescence signal. We also did not observe any non-specific amplification from NTC samples, which are milk samples that were not spiked with bacteria.

After confirmation of successful PCR on our device, we tested a milk sample contaminated with both *E. coli* and *S. aureus,* and this time we analyzed the PCR amplicon using the CE separation for multiplex detection. For this analysis, we used the FAM-tagged primers to obtain clear and accurate fluorescence peak signals in the electropherogram. We observed an electropherogram (Fig. 4b) showing successful multiplex PCR and clear separation of two amplicons indicating *E. coli* (earlier peak at ~158 s) and *S. aureus* (later peak at ~161 s), despite the small size difference of only 13 bp between their products (99 vs. 112 base pairs). As expected, the peak fluorescence intensity decreased linearly as the number of bacterial cells decreased 10-fold (Fig. 4c), and the lowest cell number that produced a detectable fluorescence signal was determined to be 10 cells for both *E. coli* and *S. aureus*, establishing the detection limit of our system. The R-squared values of the linear regression curves were 0.99899 for *E. coli* and 0.97821 for *S. aureus*, respectively, confirming the quantitative range within the tested concentrations of 10 to 10^3 cells.

Taken together, these results demonstrate the streamlined procedures and device architecture required for genetic analysis as the direct PCR technique enabled us to skip the extensive sample preparation steps for DNA extraction and purification. While these results establish the viability of performing molecular assays, traditionally confined to laboratory environments, in decentralized POC settings, our device's practical implementation may face certain challenges associated with the diversity of sample types. Our device supports a variety of direct PCR kit protocols without necessitating modifications to its architecture, but its performance can be influenced by the nature of the sample. For instance, liquid biological samples, e.g., blood, saliva, and urine, are readily compatible with our system; however, for samples with high cellular integrity or rigid structures, such as tissue or environmental specimens, additional sample preparation steps, including enzymatic digestion or mechanical disruption, may be necessary to ensure effective lysis. Consequently, the overall processing time and analytical performance of our device are contingent upon the sample type, underscoring the importance of tailoring workflows to specific applications.

4. Conclusion

In this study, we developed a simple microfluidic device that leveraged direct PCR technology to streamline the PCR process and device architecture for rapid detection of pathogens. Compared to traditional PCR methods, our device eliminates the need for DNA extraction and purification steps, significantly reducing operational complexity, time, and contamination risks. Furthermore, unlike other microfluidic PCR devices, which often rely on intricate valve systems, external pumps, and tubing, our design incorporates a slidable microchamber for seamless sample transfer, minimizing the need for external equipment. These attributes make our device particularly advantageous for POC applications, enabling rapid and reliable molecular diagnostics with minimal training, whereas its cost-effective and scalable operation is suitable for decentralized and resource-limited settings.

While we demonstrated the device's capability by detecting and quantifying both *E. coli and S. aureus* in milk samples at concentrations as low as 10 cells, its potential extends to the molecular diagnosis of other pathogenic targets, such as SARS-CoV-2, influenza virus, Zika virus, hepatitis B virus, or malaria. In addition, without requiring modifications to the device design or assay protocol, it can accommodate various direct PCR kits, effectively managing variations in amplification conditions or reaction times to

ensure flexibility and adaptability for different sample types. Considering the growing importance of accessible and efficient PCR diagnostics, this work demonstrates how the integration of direct PCR with a streamlined microfluidic platform can overcome existing limitations, making traditionally labor-intensive molecular assays available in a decentralized POC setting.

CRediT authorship contribution statement

Dohwan Lee: Writing – review & editing, Writing – original draft, Visualization, Validation, Resources, Methodology, Investigation, Formal analysis, Data curation, Conceptualization. **Tae Seok Seo:** Writing – review & editing, Resources, Project administration, Funding acquisition, Conceptualization.

Declaration of competing interest

The authors declare that they have no known competing financial interests or personal relationships that could have appeared to influence the work reported in this paper.

Acknowledgments

The present Research has been conducted by the Research Grant of Kwangwoon University in 2024. This work was also supported by the National Research Foundation of Korea (NRF), Ministry of Science and ICT (MSIT) (2020R1A2C1003960) and the Ministry of Health and Welfare of South Korea (HI22C0426).

Appendix A. Supplementary data

Supplementary data to this article can be found online at https://doi.org/10.1016/j.heliyon.2025.e42183.

References

[1] R. Wölfel, V.M. Corman, W. Guggemos, M. Seilmaier, S. Zange, M.A. Müller, D. Niemeyer, T.C. Jones, P. Vollmar, C. Rothe, et al., Virological assessment of hospitalized patients with COVID-2019, Nature 581 (2020) 465–469.
[2] B. Udugama, P. Kadhiresan, H.N. Kozlowski, A. Malekjahani, M. Osborne, V.Y.C. Li, H. Chen, S. Mubareka, J.B. Gubbay, W.C.W. Chan, Diagnosing COVID-19 : the disease and tools for detection, ACS Nano 14 (2020) 3822–3835.
[3] P.B. van Kasteren, B. van der Veer, S. van den Brink, L. Wijsman, J. de Jonge, A. van den Brandt, R. Molenkamp, C.B.E.M. Reusken, A. Meijer, Comparison of seven commercial RT-PCR diagnostic kits for COVID-19, J. Clin. Virol. 128 (2020) 104412.
[4] L.J. Carter, L.V. Garner, J.W. Smoot, Y. Li, Q. Zhou, C.J. Saveson, J.M. Sasso, A.C. Gregg, D.J. Soares, T.R. Beskid, et al., Assay techniques and test development for COVID-19 diagnosis, ACS Cent. Sci. 6 (2020) 591–605.
[5] D. Lee, C.H. Chu, A.F. Sarioglu, Point-of-Care toolkit for multiplex molecular diagnosis of SARS-CoV-2 and influenza A and B viruses, ACS Sens. 6 (2021) 3204–3213.
[6] Y. Woodbridge, Y. Goldberg, S. Amit, N.M. Kopelman, M. Mandel, A. Huppert, Public health-focused use of COVID-19 rapid antigen and PCR tests, Sci. Rep. 14 (2024) 1430.
[7] T. Tamaki, W. Nozawa, A. Kitsuki, How did you perceive the lifestyle changes caused by the COVID-19 pandemic? Humanit. Soc. Sci. Commun. 11 (2024) 70.
[8] P.N. Barbieri, O. Giuntella, S. Saccardo, S. Sadoff, Lifestyle and mental Health 1 Year into COVID-19, Sci. Rep. 11 (2021) 23349.
[9] P. Elliott, O. Eales, N. Steyn, D. Tang, B. Bodinier, H. Wang, J. Elliott, M. Whitaker, C. Atchison, P.J. Diggle, et al., Twin peaks: the omicron SARS-CoV-2 BA.1 and BA.2 epidemics in england, Science 376 (2022) 1432.
[10] O.I. Wilner, D. Yesodi, Y. Weizmann, Point-of-Care nucleic acid tests: assays and devices, Nanoscale 15 (2023) 942–952.
[11] M.G. Rizzo, S. Carnazza, L.M. De Plano, D. Franco, M.S. Nicolò, V. Zammuto, S. Petralia, G. Calabrese, C. Gugliandolo, S. Conoci, et al., Rapid detection of bacterial pathogens in blood through engineered phages-beads and integrated real-time PCR into MicroChip, Sensor. Actuator. B Chem. 329 (2021) 129227.
[12] J. Yin, J. Tong, J. Li, G. Shao, B. Xie, J. Zhuang, G. Bi, Y. Mu, A portable, high-throughput real-time quantitative PCR device for point-of-care testing, Anal. Biochem. 674 (2023) 115200.
[13] J. Caffry, M. Selby, K. Barr, G. Morgan, D. McGurk, P. Scully, C. Park, A.M. Caridis, E. Southworth, J. Morrison, et al., The QuantuMDx Q-POC SARS-CoV-2 RT-PCR assay for rapid detection of COVID-19 at point-of-care: preliminary evaluation of a novel technology, Sci. Rep. 13 (2023) 9827.
[14] Q. Song, X. Sun, Z. Dai, Y. Gao, X. Gong, B. Zhou, J. Wu, W. Wen, Point-of-Care testing detection methods for COVID-19, Lab Chip 21 (2021) 1634–1660.
[15] H.Q. Nguyen, V.D. Nguyen, V.M. Phan, T.S. Seo, A novel point-of-care platform for rapid SARS-CoV-2 detection utilizing an all-in-one 3D-printed microfluidic cartridge and IoT technology, Sensor. Actuator. B Chem. 410 (2024) 135632.
[16] H.K. Bui, V.M. Phan, H.Q. Nguyen, V.D. Nguyen, H. Van Nguyen, T.S. Seo, Function of the speech recognition of the smartphone to automatically operate a portable sample pretreatment microfluidic system, ACS Sens. 8 (2023) 515–521.
[17] D. Lee, Y.T. Kim, J.W. Lee, D.H. Kim, T.S. Seo, An integrated direct loop-mediated isothermal amplification microdevice incorporated with an immunochromatographic strip for bacteria detection in human whole blood and milk without a sample preparation step, Biosens. Bioelectron. 79 (2016) 273–279.
[18] D. Lee, T. Ozkaya-Ahmadov, C.H. Chu, M. Boya, R. Liu, A.F. Sarioglu, Capillary flow control in lateral flow assays via delaminating timers, Sci. Adv. 7 (2021) eabf9833.
[19] H. Van Nguyen, V.M. Phan, T.S. Seo, High-throughput centrifugal microfluidic platform for multiplex respiratory virus diagnostics, Sensor. Actuator. B Chem. 399 (2024) 134771.
[20] V.D. Nguyen, H.Q. Nguyen, H.K. Bui, Y.J. Kang, T.S. Seo, A smartphone-controllable molecular diagnostic platform for SARS-CoV-2 detection by reverse-transcription recombinase polymerase amplification, Sensor. Actuator. B Chem. 398 (2024) 134728.
[21] N. Wang, J. Zhang, B. Xiao, A. Chen, Microfluidic-assisted integrated nucleic acid test strips for POCT, Talanta 267 (2024) 125150.
[22] V. Garzarelli, M.S. Chiriacò, M. Cereda, I. Autuori, F. Ferrara, Miniaturized real-time PCR systems for SARS-CoV-2 detection at the point-of-care, Clin. Chim. Acta 536 (2022) 104–111.

[23] P. Zhang, L. Chen, J. Hu, A.Y. Trick, F.E. Chen, K. Hsieh, Y. Zhao, B. Coleman, K. Kruczynski, T.R. Pisanic, et al., Magnetofluidic immuno-PCR for point-of-care COVID-19 serological testing, Biosens. Bioelectron. 195 (2022) 113656.
[24] L. Xu, H. Qu, D.G. Alonso, Z. Yu, Y. Yu, Y. Shi, C. Hu, T. Zhu, N. Wu, F. Shen, Portable integrated digital PCR system for the point-of-care quantification of BK virus from urine samples, Biosens. Bioelectron. 175 (2021) 112908.
[25] M.I. Mohammed, S. Haswell, I. Gibson, Lab-on-a-Chip or chip-in-a-lab: challenges of commercialization lost in translation, Procedia Technol 20 (2015) 54–59.
[26] S. Dekker, P.K. Isgor, T. Feijten, L.I. Segerink, M. Odijk, From chip-in-a-lab to lab-on-a-chip: a portable coulter counter using a modular platform, Microsystems Nanoeng 4 (2018) 34.
[27] M.I. Mohammed, A lab-on-a-chip that takes the chip out of the Lab, Nature 605 (2022) 429–430.
[28] M. Yafia, O. Ymbern, A.O. Olanrewaju, A. Parandakh, A.S. Kashani, J. Renault, Z. Jin, G. Kim, A. Ng, D. Juncker, Microfluidic chain reaction of structurally programmed capillary flow events, Nature 605 (2022) 464–469.
[29] D. Lee, Y.T. Kim, J.W. Lee, D.H. Kim, T.S. Seo, An integrated slidable direct polymerase chain reaction-capillary electrophoresis microdevice for rapid Y chromosome short tandem repeat analysis, Kor. J. Chem. Eng. 33 (2016) 2644–2649.
[30] S.E. Cavanaugh, A.S. Bathrick, Direct PCR amplification of forensic touch and other challenging DNA samples: a review, Forensic Sci. Int. Genet. 32 (2018) 40–49.
[31] B. Martin, A. Linacre, Direct PCR: a review of use and limitations, Sci. Justice 60 (2020) 303–310.
[32] B. Martin, D. Taylor, A. Linacre, Comparison of six commercially available STR kits for their application to touch DNA using direct PCR, Forensic Sci. Int. Reports 4 (2021) 100243.
[33] A. Castellanos-Gonzalez, T.R. Shelite, N. Lloyd, A. Sadiqova, R. Ping, N. Williams-Bouyer, P.C. Melby, B.L. Travi, Direct RT-PCR amplification of SARS-CoV-2 from clinical samples using a concentrated viral lysis-amplification buffer prepared with IGEPAL-630, Sci. Rep. 11 (2021) 14204.
[34] M. Aslam, R. Seher, M.Z. Shabbir, W. Shehzad, M. Imran, Direct PCR assays for DNA barcoding and sexing of plucked feathers, Gene Reports 36 (2024) 101937.
[35] Y.Y. Kim, D. Lee, H.Y. Heo, D.H. Kim, T.S. Seo, An integrated slidable and valveless microdevice with solid phase extraction, polymerase chain reaction, and immunochromatographic strip parts for multiplex colorimetric pathogen detection, Lab Chip 15 (2015) 4148–4155.
[36] Y.T. Kim, J.Y. Choi, Y. Chen, T.S. Seo, Integrated slidable and valveless polymerase chain reaction–capillary electrophoresis microdevice for pathogen detection, RSC Adv. 3 (2013) 8461–8467.